Cation intercalation in sputter-deposited W oxide films

Maria Strømme Mattsson
Department of Materials Science, The Ångström Laboratory, Uppsala University, P.O. Box 534, S-751 21 Uppsala, Sweden
(Received 27 April 1998)

Intercalation of Li, Na, and K ions into sputtered amorphous and monoclinic W oxide has been studied electrochemically and by x-ray diffraction. It was found that both Li and K intercalation, at low concentrations, caused a phase separation in the crystalline W oxide, while Na intercalation, at low concentrations, accurately followed the lattice-gas model [A. J. Berlinsky, W. G. Unruh, W. R. McKinnon, and R. R. Haering, Solid State Commun. **31**, 135 (1979)]. The lattice-gas model was also used to extract information about the electrochemical response at high concentrations of all three types of intercalants. At low concentrations the net interaction between the intercalated ions was found to be attractive, while at higher concentrations the interaction was repulsive. Intercalation of alkali ions into amorphous W oxide could be modeled with a Gaussian distribution of site energies. The distribution of Li ions was found to be narrower and peaked at a lower energy than that of Na and K ions. [S0163-1829(98)01240-5]

I. INTRODUCTION

Tungsten trioxide is by far the most extensively studied working electrode material for electrochromic devices.[1] The initially transparent W oxide darkens when ions such as H^+, Li^+, Na^+, and K^+ are intercalated. For disordered (or amorphous) films, polaron absorption is believed to be responsible for the observed electrochromism.[1] In this picture the electrons that are inserted to charge-balance the inserted cations occupy localized states on tungsten sites, rather than entering empty states in electron bands. In crystalline films the electrochromism is most likely due to free-electron effects and can be understood schematically by Drude theory, in which the inserted electrons enter extended states in the WO_3 band structure and undergo scattering by impurities.[1]

The physical properties of an intercalation material are to a great extent unveiled by the voltage versus composition relationship. By measuring the voltage as a function of the amount of intercalated ions and electrons, one can get information about, e.g., phase changes,[2] electron density of states,[3] interactions between the intercalated ions and between the ions and the host,[4] and also about the difference in energy between available sites for the ions to reside in.[5] Some information has been extracted earlier from voltage versus composition curves recorded on either amorphous (see, e.g., Ref. 6) or crystalline (see, e.g., Ref. 2) W oxide under intercalation of one chosen cationic species.

The aim of this paper is to study the voltage versus composition response of sputtered amorphous and crystalline W oxide under intercalation of Li, Na, and K ions, and to determine parameters describing the physics of the intercalation system. To accomplish this, the Kudo model[7] and the lattice-gas model[4,5] are used together with *ex situ* x-ray diffraction (XRD) measurements.

The paper is organized as follows: film preparation and characterization are recapitulated in Secs. II and III, respectively. In Sec. IV, the electrochemical measurements with accompanying XRD measurements are described. Section V deals with the theoretical background of the lattice-gas[4,5] and the Kudo model,[7] and Sec. VI presents the results obtained by applying these models to the data obtained in Sec. IV. The paper is summarized in Sec. VII.

II. FILM PREPARATION

W oxide films were made by reactive dc magnetron sputtering in a deposition system based on a Balzers UTT 400 unit with a background pressure of 10^{-7} Torr as described in Ref. 8. Films studied by XRD and electrochemical techniques were deposited onto glass plates precoated with transparent and conducting In_2O_3:Sn (known as ITO) layers having a resistance/square of abut 15 Ω, while films investigated by Rutherford backscattering spectroscopy (RBS) were deposited onto carbon substrates. Deposition took place onto unheated substrates as well as substrates heated to 350 °C. The films deposited onto the unheated (heated) substrates had a thickness of ~285 (350) nm as measured with surface profilometry.

III. FILM CHARACTERIZATION

Structural analysis was carried out by XRD, employing a Siemens D 5000 diffractometer with a CuK_α cathode. Diffractograms for the as deposited films as well as for the ITO covered glass are shown in Fig. 1. It is readily seen that the film deposited onto the unheated substrate is amorphous; the diffraction peaks appearing for this sample are identical to those of the underlying ITO covered glass. The film deposited onto the heated substrate is monoclinic[9] with a grain size of ~50 nm as obtained from a peak profile fitting using Sherrer's equation.[10]

Composition analysis was performed by RBS at the Tandem accelerator laboratory at Uppsala University using 2 MeV alpha particles at 6° incidence. The composition of the crystalline tungsten oxide was found to be $WO_{3.1}$, while the amorphous film had an oxygen to tungsten ratio of 3.23. The high oxygen content of the amorphous film is most likely due to water incorporated while storing in air.[1] The water uptake in the crystalline film being lower than in the amorphous one can probably be understood from the difference in

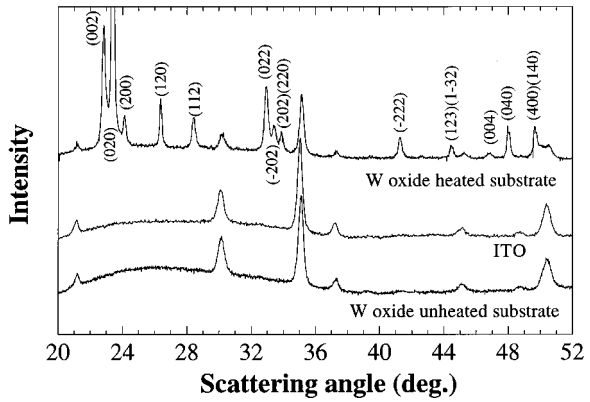

FIG. 1. X-ray diffractograms for as deposited W oxide films and for ITO covered glass. The indexed peaks are those of the monoclinic phase (Ref. 9).

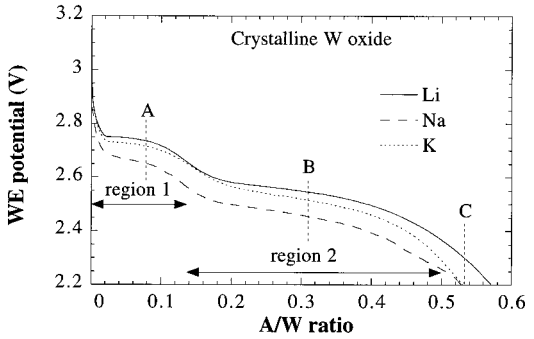

FIG. 2. The WE potential as a function of the A/W ratio x (A is Li, Na, or K) as obtained under constant current intercalation into crystalline W oxide. Points A–C indicate the compositions at which XRD measurements were made. The two regions marked out are used in the analysis below.

film density. The density of the crystalline and amorphous sample as obtained from the number of atoms per cm^2 and the film thickness was 6.44 and 5.60 $\mathrm{g/cm}^3$, respectively, which is ~90 and 78 % of the theoretical bulk density of monoclinic WO_3.[1]

IV. CHRONOPOTENTIOMETRY MEASUREMENTS WITH *ex situ* XRD

For the electrochemical measurements, a standard three-electrode arrangement[11] was employed with the W oxide film as working electrode (WE), and with carbon (rigid graphite) and metallic lithium foil as counterelectrode and reference electrode, respectively. The electrodes were immersed in an electrolyte of 1 M $A\mathrm{ClO}_4$ (with A being Li, Na, or K) in propylene carbonate, and the experiments were conducted in an atmosphere containing less than 0.6 ppm of water (dew point below $-80\,^{\circ}\mathrm{C}$).

The variation of the WE potential with changing cation content in the films was studied by intercalating ions at a constant current of ~30 $\mathrm{mA/cm}^3$ (which is equivalent to ~1 μA per cm^2 for the crystalline films), using an ECO Chemie Autolab/GPES electrochemical interface. The reaction describing the intercalation/deintercalation of cations A may be represented, schematically, as[1]

$$\mathrm{WO}_3\,(\text{transparent}) + xA^+ + xe^- \leftrightarrow A_x\,\mathrm{WO}_3\,(\text{blue}), \quad (1)$$

where e^- denotes charge-balancing electrons. The WE potential as a function of the A/W ratio x is displayed in Figs. 2 and 3 for the crystalline and amorphous samples, respectively. The ratio x is determined from time, intercalation current, film surface area, and the number of W atoms per surface area (obtained by RBS). When calculating x from these parameters, and not using the film density, one avoids errors due to film thickness uncertainties. The chronopotentiometry curves of intercalation into the crystalline samples (Fig. 2) show some structure with two more or less flat regions in the displayed potential range, while the corresponding curves for the amorphous films (Fig. 3) are featureless with the WE potential decreasing with increasing cation content.

To be sure that the curves in Figs. 2 and 3 represent close-to-equilibrium data, the intercalation (discharge) was made at different currents. It was found that kinetic effects were negligible (the potential curves were identical) for currents of ~30 $\mathrm{mA/cm}^3$ and smaller. Using currents low enough to ensure quasiequilibrium is very important for the correctness of the analysis to follow.

Crystalline W oxide samples were intercalated to the three different A/W ratios specified by the points A–C in Fig. 2, and *ex situ* XRD measurements were made in air during 12 h. The diffractograms are shown in Fig. 4. When interpreting the diffractograms, one must be aware of the possibility of ion leakage during the XRD measurements.

The structures of tungsten bronzes have been studied by Hägg and Magneli[12] and many others. They found that (i) the symmetry of the structure $A_x\mathrm{WO}_3$ increases with increasing x, (ii) the structure depends on the ionic radius of A, and (iii) all the structure are based on WO_6 octahedra sharing corners or edges. Considering the diffractograms of the as deposited W oxide in Fig. 1 and those of intercalated W oxide in Fig. 4, we see that the general feature is that the number of diffraction peaks decreases with increasing A/W ratio, thus indicating an increasing symmetry of the structure in accordance with the observation of Hägg and Magneli.[12]

The Li containing W oxide samples seem to go through structural changes similar to those observed by Zhong, Dahn, and Colbow.[2] This is seen by comparing the peak positions and relative intensities to those in Ref. 2. From this comparison it is evident that points A, B, and C on the whole, can be related to a monoclinic, tetragonal, and cubic structure, respectively. The structures are not completely pure, but con-

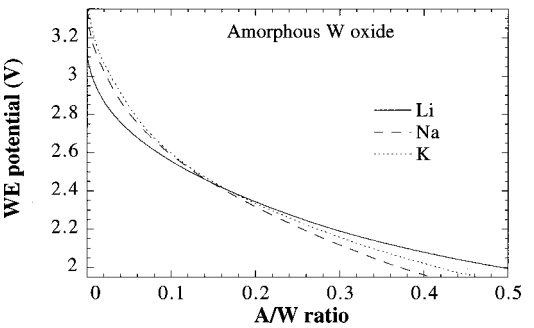

FIG. 3. The WE potential as a function of the A/W ratio x (A is Li, Na, or K) as obtained under constant current intercalation into amorphous W oxide.

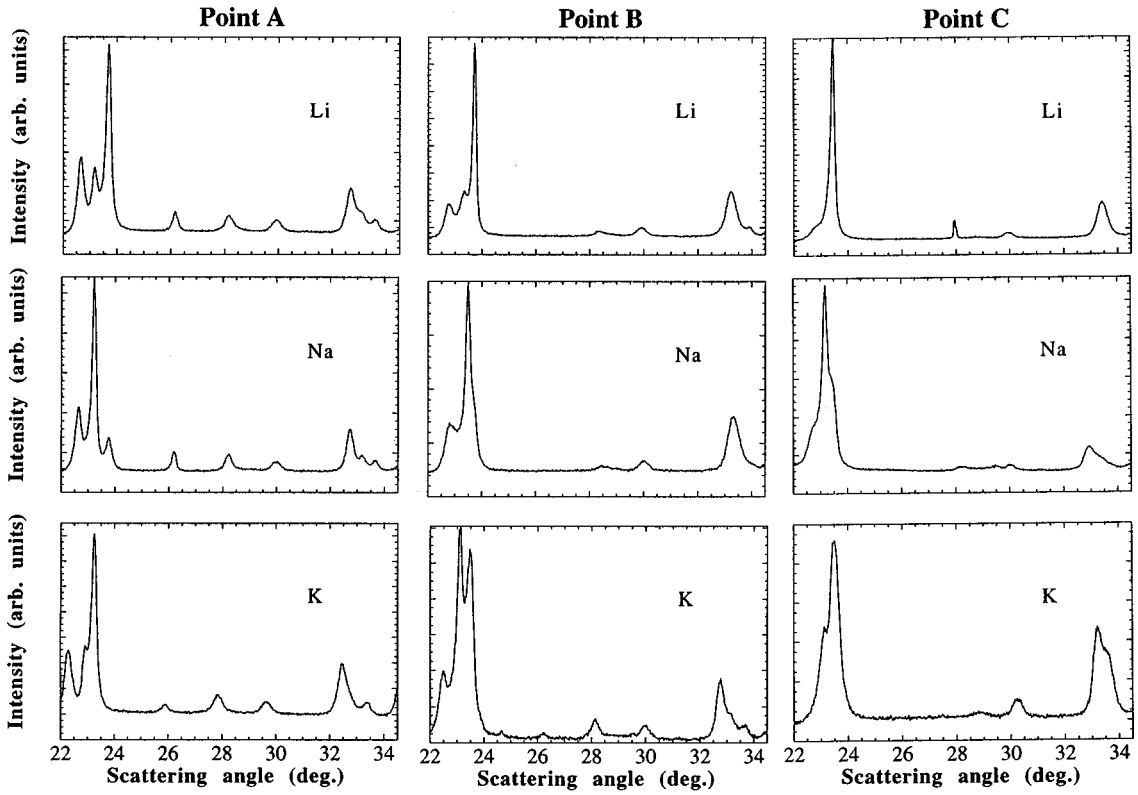

FIG. 4. X-ray diffractograms recorded in air on W oxide films intercalated with the indicated type of ion. The compositions are specified by points *A*, *B*, and *C* in Fig. 2.

tain features suggesting that additional phases are present, either due to ion leakage or to a real two-phase situation, as discussed below.

Consider now the change in the peaks appearing at scattering angles of 32°–34° in the Li panels of Fig. 4. The monoclinic phase (Fig. 1) has three distinct peaks here, while the tetragonal and cubic phases have two and one peak, respectively, in this region.[2] In the Li panel at point *A* in Fig. 4 there are three peaks between the scattering angles 22° and 24° and two peaks between 25° and 29°, just as in the as deposited monoclinic film (cf. Fig. 1). Between 32° and 34°, however, we see three peaks that are much less distinct than in the as deposited film, indicating an overlap between a phase with two peaks (tetragonal) and one with three peaks (monoclinic). A similar observation was made by Zhong, Dahn, and Colbow[2] and their conclusion was that the Li containing W oxide consisted of two phases (monoclinic and tetragonal) at intercalation levels corresponding to point *A* in Fig. 2. They also found that Li containing W oxide was two-phase (tetragonal and cubic) at intercalation levels corresponding to point *B*. One must be careful to draw the same conclusion from the present data, though, due to the above-mentioned possibility of ion leakage while running the XRD measurements in air. If a small part of the sample under study contains less ions than was electrochemically intercalated before the sample was placed in the XRD unit, it will seem as if two (or more) phases coexist even if the sample was one-phase right after removing it from the electrolyte. So the x-ray diffractograms presented here should not be used for a detailed investigation of the W oxide structure, but rather as a support for the electrochemical analysis to follow and to—in rough outlines—give a picture of what is happening in the W oxide host during intercalation.

The Na and K containing W oxide samples (Fig. 4) seem to go through structural changes similar to those of the Li containing film. The analysis of the electrochemical data presented in Sec. VI below, will give an indication as to whether the samples are one- or two-phase in the two regions marked out in Fig. 2.

V. THEORY

A. Lattice-gas model: Crystalline host

A model describing the voltage-composition relationship can be derived from statistical mechanics. Assuming that ions are intercalated randomly into equivalent sites and that each intercalated ion is exposed to a mean interaction or field from its intercalated neighbors, the WE potential V_{WE} can be expressed as[5]

$$V_{\mathrm{WE}}=\varepsilon+kT\ln\left(\frac{1-y}{y}\right)-Uy+V_{\mathrm{electrons}}, \tag{2}$$

where the first term is the site energy, the second term is the entropy of ions, the third term is the ion interactions, and the fourth is interactions and entropy due to electrons. Here ε, the site energy, is the potential (or the energy in electron volts) required to put an isolated ion and its electron into the host, k is Boltzmann's constant, and T the temperature. The ions occupy a fraction y of all available and energetically

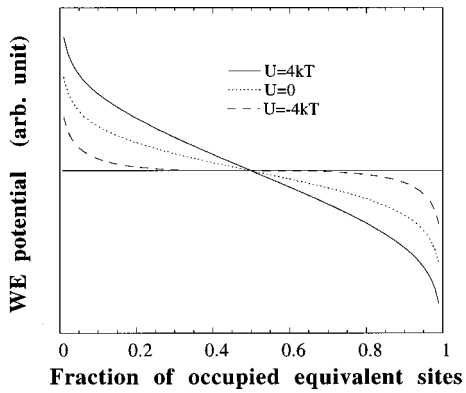

FIG. 5. WE potential vs the fraction of energetically equivalent sites occupied by inserted ions, as given by the lattice-gas model. The response is shown for three different values of the interaction parameter U. kT is Boltzmann's constant times temperature.

equivalent sites in the host. U is the total interaction potential (or energy) that an intercalated ion would experience if all the other sites were full; hence U includes both the repulsive Coulombic interactions between intercalated ions and strain fields caused by expansion or contraction of the lattice. $V_{\text{electrons}}$ denotes the electronic contribution to the potential.

The electronic contribution to the potential may be complex, but at least for metallic compounds one can argue[5] that the $V_{\text{electrons}}$ term may be neglected. Crystalline W oxide films become metallic under intercalation,[1] so the $V_{\text{electrons}}$ term is omitted to simplify the analysis.

The interaction parameter U can give us information about whether the net force on an intercalated ion tends to attract it towards (negative U) or repel it from (positive U) other intercalated ions, and whether this force is strong or weak.[5] It also provides information about the approximate temperature at which phase separations can be expected.[13] Thermodynamics requires that the chemical potential μ increase with concentrations of intercalated ions, so V_{WE}—which is proportional to $-\mu$—must decrease. Mathematically this means that

$$\frac{dV_{\text{WE}}}{dy}<0. \tag{3}$$

Inequality (3) gives that U must be larger than $-4kT$. Systems with stronger attractive forces (more negative U value) will separate into a two-phase mixture with a composition-independent V_{WE}.[14] Likewise, for temperatures lower than a critical temperature $T_c=-U/4k$, the system will phase separate. Figure 5 displays Eq. (2) for three different U values, and the typical s-shaped curves of the lattice-gas model are visible. We also see that the more negative U is, the flatter the response becomes.

To obtain an equation that can be used in practice to fit the experimental curves in Fig. 2, the parameter x (the number of intercalated species per W atom) must be related to the parameter y in Eq. (2). The figure marks *two* regions in whose center the potential curves have a small slope. The magnitude of the voltage is mainly determined by the site energy ε,[5] so the two regions represent two different types of sites for the ions to reside in. The x-ray diffractograms (Fig. 4) indicate that region 1 represents intercalation into sites in the monoclinic structure and region 2 into a tetragonal structure. By introducing two parameters, x_0 and x_1, the lattice-gas model can be applied to each region separately. With x_0 being the number of intercalated ions per W before starting to fill the type of site under study and x_1 being that number when this type of site is full, one gets that $y=x-x_0/x_1-x_0$. Rewriting Eq. (2) gives

$$V_{\text{WE}}=\varepsilon+kT\ln\left(\frac{x_1-x}{x-x_0}\right)-U\frac{x-x_0}{x_1-x_0}. \tag{4}$$

B. The Kudo model: amorphous host

The former section was devoted to intercalation systems where one can assume that the ions are intercalated into equivalent sites, which may be the case for crystalline samples. Although the equivalency of sites is one of the requirements for the lattice-gas model to be applicable, several studies on amorphous hosts have used this model and found repulsive energies described by U values as large as $\sim 20kT$.[6,15] Kudo and Hibino[7] showed that the steep potential-composition curves (cf. Fig. 3 and figures in Refs. 6 and 15) of most amorphous compounds could not be explained by large repulsive energies but rather by a relatively wide distribution of site energies. Neglecting the repulsive interactions and assuming that the site energies in the amorphous host had a Gaussian distribution with a standard deviation σ, an equation for fitting the amorphous potential-composition curves was derived to yield[7]

$$V_{\text{WE}}=-\left[E_0+\sqrt{2}\sigma\,\text{erf}^{-1}(2x-1)+kT\ln\left(\frac{\xi(1-x)}{x(1-2x+\xi)}\right)\right]. \tag{5}$$

The parameter E_0 denotes the mean energy in the distribution, and erf^{-1} is the inverse error function. The parameter ξ is the ratio of the number of ion pairs occupying neighboring sites to the number of available sites, as worked out and explained in more detail in Ref. 7. In this work ξ is only used as a fitting parameter.

VI. RESULTS AND DISCUSSION

The lattice-gas model [Eq. (4)] was compared with the chronopotentiometry curves in Fig. 2. One fit was made for each of the two composition regions discussed at the end of Sec. V A. The result is displayed in Fig. 6. To get a better picture of the quality of the fits, the derivative $-(dx/dV_{\text{WE}})$ is plotted versus x in Fig. 7.

We first concentrate on intercalation in region 1 (i.e., low concentration of intercalants). From Figs. 6(a) and 6(c) and Figs. 7(a) and 7(c), it can be seen that the lattice-gas model does not describe the intercalation of Li and K particularly well. The measured $-(dx/dV_{\text{WE}})$ for these ions are not very symmetric, and the peak values are higher than those obtained in the best fits [the squares in Figs. 7(a) and 7(c)] to the lattice-gas model. The fact that the maximum values of the measured $-(dx/dV_{\text{WE}})$ curves are larger than those from the lattice-gas model means that the recorded potential versus composition curves are sloping less than the calculated ones [cf. Figs. 6(a) and 6(c)]. This implies that the values of the interaction energy U, in reality, are more negative than

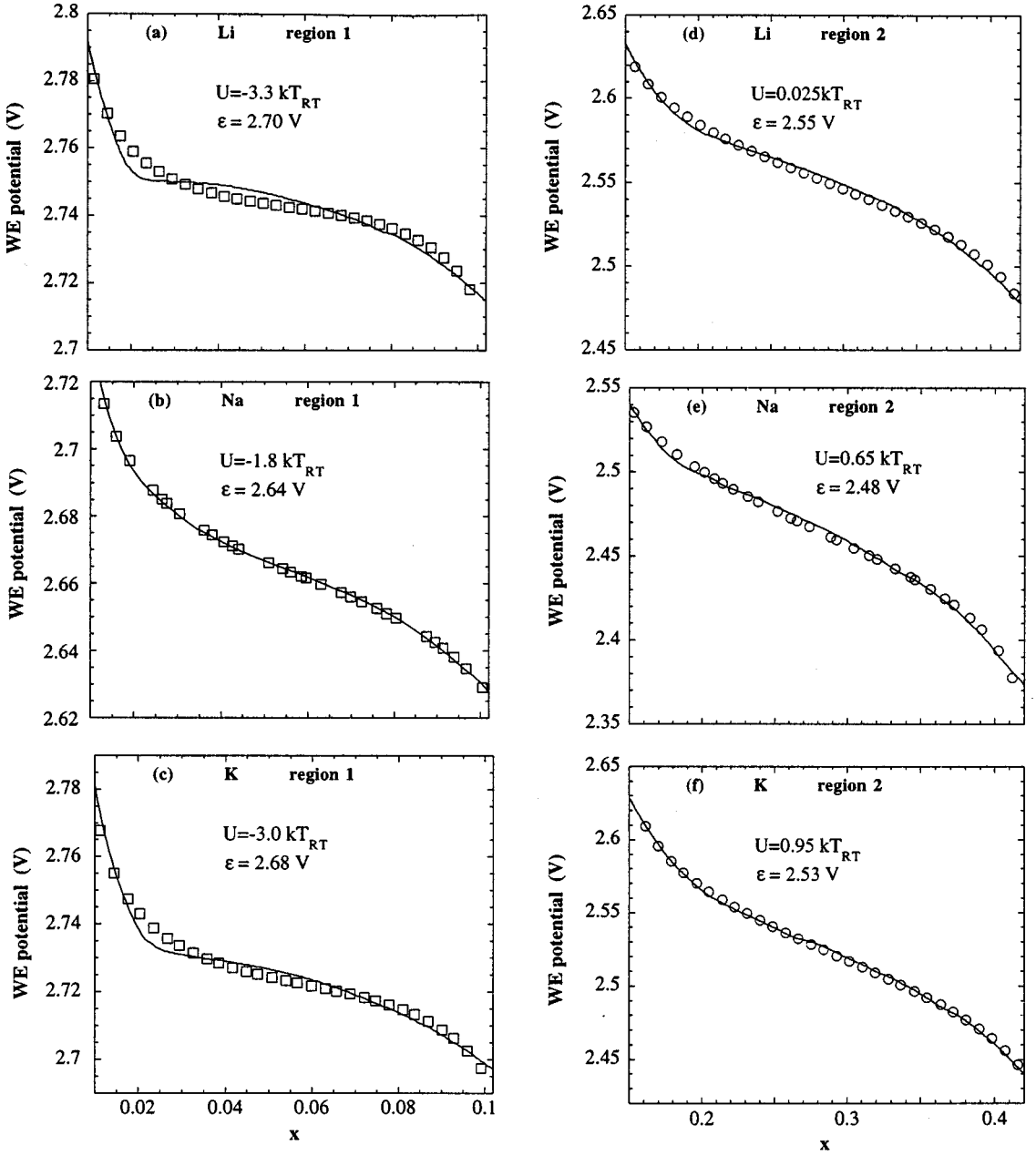

FIG. 6. WE potential vs composition x for crystalline W oxide. Full lines represent measured chronopotentiometry response (from Fig. 2). Squares (composition region 1) and circles (composition region 2) are data obtained by fitting to the lattice-gas model [Eq. (4)]. The pertinent interaction parameter U and the site energy ε are displayed. T_{RT} denotes room temperature. x is the ratio of intercalated ions to the number of W atoms.

what was obtained by the fits. Since the U values [Figs. 6(a) and 6(c)] are close to the critical value $-4kT$, the failure of the lattice-gas model is most likely due to a two-phase separation in region 1 for Li and K intercalation.

Next considering Na intercalation in region 1, one finds that the theoretical data are indistinguishable from the measured voltage curve [Fig. 6(b)]. Also the fitted and measured $-(dx/dV_{WE})$ data [Fig. 7(b)] are matching to within experimental uncertainties. Consequently the intercalation process can be accurately described by the lattice-gas model.

Looking back at the x-ray diffractograms recorded for a composition in region 1 (point A of Fig. 4), we notice that between 32° and 34° the Li and K curves show an overlap between a three-peak (monoclinic) and two-peak (tetragonal) phase, while the Na data reveal three distinct peaks here. We also observe that the relative intensities of the three peaks between 22° and 24° have changed for the Li and K containing W oxide as compared to the as-deposited film (Fig. 1). In the monoclinic phase the mid peak is the strongest,[9] while in the tetragonal phase the right peak dominates.[2] So the XRD data support the above-obtained results: For low concentrations of Li and K in crystalline W oxide, the net interactions between the intercalants are strongly attractive and the material therefore is two-phase during intercalation. This implies that the host consists of small domains of the two phases. Increasing x causes the domains of the phase with larger composition (tetragonal) to grow at the expense of the phase of lower composition (monoclinic). This is a so-called

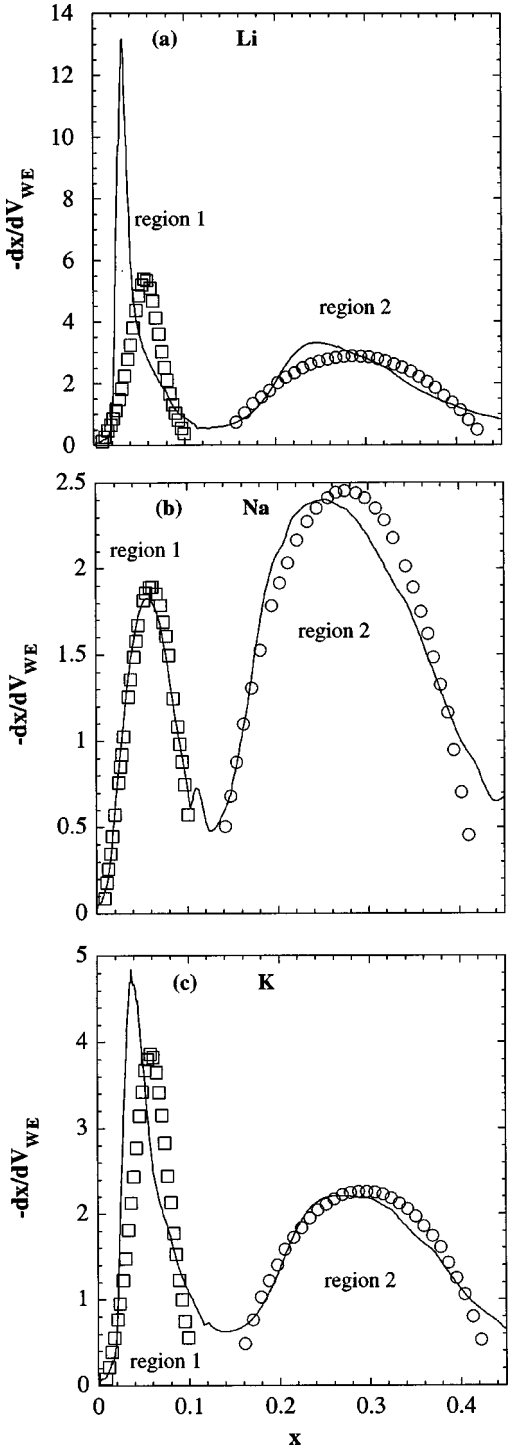

FIG. 7. Derivative of the composition x with respect to working electrode (WE) potential V_{WE}. Full lines represent measured chronopotentiometry response. The squares (composition region 1) and the circles (composition region 2) are data obtained by fitting to the lattice-gas model [Eq. (4)]. x is the ratio of intercalated ions to the number of W atoms.

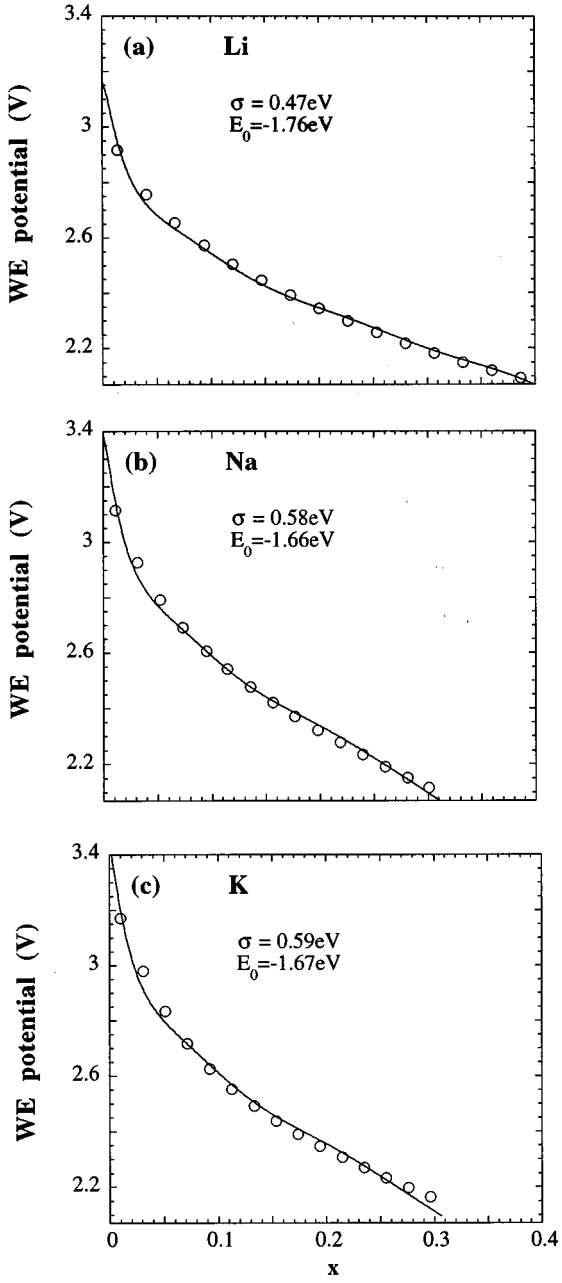

FIG. 8. WE potential vs composition x for amorphous W oxide. Circles represent measured chronopotentiometry response (from Fig. 3) and full lines are data obtained by fitting to the Kudo model [Eq. (5)]. The standard deviation σ and the mean energy value E_0 of the site energy distribution are displayed. x is the ratio of intercalated ions to be number of W atoms.

first-order phase transition.[5] For low concentrations of Na in crystalline W oxide, the net interactions between the Na ions are attractive, $U=-1.8kT$ at room temperature, but not strong enough to cause phase separation. So the phase transition from a monoclinic to a tetragonal structure is continuous in the Na case.

From Figs. 6(d)–6(f), it seems as if the lattice-gas model describes intercalation in the high-concentration region (region 2) well. Figure 7, however, shows that the matching between the measured and the calculated data in this region are not as good as for Na intercalation at low concentrations. The fits are somewhat better for Na and K intercalation than for Li, but the peaks for all three intercalation processes are slightly asymmetric and not exactly described by the symmetric lattice-gas model. Since the lattice-gas model used here seems to be too simple to reproduce the measured data perfectly, it could be that an electron intercalation term and/or some distribution in site energies must be included to

obtain better fits. The heights and widths of the peaks in region 2 (Fig. 7) are, however, well reproduced by the simple lattice-gas model so the fits in Figs. 6 and 7 (region 2) can be used to extract the interaction parameter U to get an idea of its sign and order of magnitude. As can be seen from Figs. 6(d)–6(f), the interaction energy is positive, i.e., the net interaction between the intercalants is repulsive. This means that the material is far from phase separating.

Before moving on to the amorphous samples, a small digression may be appropriate concerning regions 1 and 2. From Fig. 2 it is evident that region 1 is described by x values smaller than ~ 0.13, while region 2 is characterized by x values lying in the ~ 0.13 to ~ 0.5 interval. One should recall from the XRD analysis that the as-deposited W oxide sample is monoclinic and most likely becomes tetragonal upon intercalation. The monoclinic and tetragonal WO_3 structures contain 8 and 2 W atoms per cell, respectively.[9,16] This indicates that the number of sites with highest accessibility for alkali ions is one per cell ($x = 0.125$) in the as-deposited material. When one alkali ion per cell has been intercalated, the structure has become more symmetric (tetragonal) and the ions that are on their way into the material have to look for sites that are more difficult to access (represented by a lower potential) than the ones in the monoclinic structure. In the tetragonal structure it again turns out to be most advantageous to place one alkali ion in each cell ($x = 0.5$).

Considering now the amorphous samples, it was argued in Sec. V B that the lattice-gas model could not be used to extract information about the intercalation process but that instead the Kudo model[7] should be employed. Figure 8 shows Eq. (5) fitted to the experimental chronopotentiometry data recorded on amorphous W oxide. As can be seen, this model describes the measured response fairly well, which speaks in favor of a Gaussian distribution of site energies.

The calculated values of σ and E_0 for Li intercalation into the sputtered amorphous W oxide films in this work are in very good agreement with values found by Kudo and Hibino[7] for Li interaction into electron beam evaporated amorphous W oxide. They found $\sigma = 0.50$ eV and $E_0 = -1.77$ eV (Ref. 7), compared with $\sigma = 0.47$ and $E_0 = -1.76$ eV in this paper [cf. Fig. 8(a)]. It is interesting to notice that the distribution of site energies is broader for Na and K (the σ values are larger) than for Li. We also recognize that it is energetically more beneficial for Li ions to enter the host than for the larger ions; the mean site energy value E_0 for Li is lower.

VII. SUMMARY AND CONCLUDING REMARKS

In this paper, the response of the electrochemical cell voltage has been studied for Li, Na, and K ion intercalation into sputtered amorphous and monoclinic W oxide films. It was found that intercalation into the crystalline host takes place in two steps. In the first step, the concentration of intercalants is $< \sim 0.13$. According to XRD, the structure of the host is then changing from monoclinic to tetragonal in a manner described below. In the second step, the concentration of intercalants is between ~ 0.13 and ~ 0.5, and the ions are intercalated into sites in a tetragonal structure. The lattice-gas model[4,5] was applied to both steps. It was found that both Li and K intercalation caused a separation of an alkali ion-rich (tetragonal) and an alkali ion-poor phase (monoclinic) in the first step. XRD measurements supported these facts. It was also found that the lattice-gas model describes the intercalation of Na into the W oxide matrix in the low-concentration region very well. The net interaction between the intercalated Na ions was found to be attractive. To my knowledge, the only previous intercalation system where the lattice-gas model has proven to be so successful is that of Li intercalation into Mo_6Se_8 (Ref. 13).

At high concentrations of intercalants, the measured data were not symmetric enough to be perfectly matched by a simple lattice-gas model. The correspondence between the measured and calculated data was, however, found to be good enough to extract information about the sign and order of magnitude of the interaction between the intercalated ions. The net interaction was found to be repulsive.

The intercalation of alkali ions into amorphous W oxide could be modeled with a Gaussian distribution of site energies. The distribution of Li ions was found to be narrower and peaked at a lower energy than the corresponding properties of the Na and K ions.

The fact that a simple model, like the lattice-gas model used in this work, can be applied to describe an intercalation system so well as for Na at low concentrations in crystalline W oxide is interesting in many ways. First of all it lends support to the idea of the lattice-gas model as a means of describing the intercalation process. But most importantly, it offers an opportunity to investigate how ions are distributed and how they interact within the host material. I believe that testing this model on additional intercalation systems could provide further essential understanding to the intercalation process.

ACKNOWLEDGMENTS

I wish to thank Andris Azens for sputtering the films and Björgvin Hjörvarsson for performing the RBS. Nils-Olov Ersson is acknowledged for helping me with the XRD measurements and Claes-Göran Granqvist and Gunnar Niklasson for proofreading the manuscript.

[1] C. G. Granqvist, *Handbook of Inorganic Electrochemical Materials* (Elsevier, Amsterdam, 1995).

[2] Q. Zhong, J. R. Dahn, and K. Colbow, Phys. Rev. B **46**, 2554 (1992).

[3] M. Strømme Mattsson, A. Azens, G. A. Niklasson, C. G. Granqvist, and J. Purans, J. Appl. Phys. **81**, 6432 (1997).

[4] A. J. Berlinsky, W. G. Unruh, W. R. McKinnon, and R. R. Haering, Solid State Commun. **31**, 135 (1979).

[5] W. R. McKinnon, in *Solid State Electrochemistry*, edited by P. G. Bruce (Cambridge University Press, Cambridge, 1995), Chap. 7.

[6] R. S. Crandall, P. J. Wojtowicz, and B. W. Faughnan, Solid State Commun. **18**, 1409 (1976).
[7] T. Kudo and M. Hibino, Solid State Ionics **84**, 65 (1996).
[8] A. Azens, C. G. Granqvist, E. Pentjuss, J. Gabrusenoks, and J. Barczynska, J. Appl. Phys. **78**, 1968 (1995).
[9] JCPDS, International Centre for Diffraction Data, file no. 43-1035 (1996).
[10] H. P. Klug and L. E. Alexander, *X-ray Diffraction Procedures for Polycrystalline and Amorphous Materials* (Wiley, New York, 1974).
[11] D. K. Gosser, Jr., *Cyclic Voltammetry: Simulation and Analysis of Reaction Mechanisms* (VCH, New York, 1993).
[12] G. Hägg and A. Magneli, Rev. Pure Appl. Chem. (Australia) **4**, 235 (1954).
[13] S. T. Coleman, W. R. McKinnon, and J. R. Dahn, Phys. Rev. B **29**, 4147 (1984).
[14] K. West, B. Zachau-Christiansen, T. Jacobsen, and S. Skaarup, in *Solid State Ionics II*, edited by G.-A. Nazri, D. W. Shriver, R. A. Huggins, and M. Balkanski (Materials Research Society, Pittsburgh, 1991), p. 449.
[15] O. Bohnke and M. Rezrazi, Mater. Sci. Eng., B **13**, 323 (1992).
[16] JCPDS, International Centre for Diffraction Data, file no. 18-1417 (1996).